Line Reactance Criteria for Minimizing Line Current Harmonic Content in Diode Rectifier Connected Wind Generator Systems

Maarten J. Kamper, Christopher Africa, Casper J. J. Labuschagne and Lethiwe P. Mdakane
Department of Electrical and Electronic Engineering
Stellenbosch University
South Africa
kamper@sun.ac.za

***Abstract*—An analysis method to ensure sinusoidal currents in wind generators that are directly connected to diode rectifiers in DC wind energy systems is considered in this paper. A simple analytic calculation method is introduced whereby the harmonic generator line currents can be calculated. This method is used to identify the necessary per unit line reactance values to ensure a low harmonic current content. It is found that 0.8 per unit reactance reduces the 5th harmonic line current to 5 % of the fundamental. It is further found that multi-phase generator systems show no advantage in this regard.**

Keywords—diode rectifier, harmonic currents, wind generator, passive compensation

I. INTRODUCTION

Wind energy continues to form an integral part of the renewable energy mix in the world today. Of all installed wind energy systems, DFIG wind generators that are directly connected to the AC-grid are by far the most common. There is, however, an increase in the use of full-rated power converters as an interface between the AC-generator and the AC- or DC-grid [1]. In recent developments, DC-grids and transmissions are used in high power wind energy systems due to the efficiency it offers in the interconnection of power networks, long distance power delivery and environmental benefits [2], [3], [4]. In some cases wind generator systems are directly connected to the DC-grid by means of full-bridge diode rectifiers [5], [6], [7].

Since diode rectifiers are expected to proliferate in near future wind energy systems, special attention needs to be paid to the harmonic generator currents caused by the rectifier. Common issues associated with such harmonic currents in wind generators are torque ripple, vibration and noise, and additional power losses [6], [8]; all which degrade the wind turbine's power quality.

To minimise the harmonic current content in diode rectifier connected wind generators, active power electronic switching at the diode bridge is usually applied. Hence, much attention in literature is paid to active compensation as a means of harmonic current control [6], [8 – 11]. Passive compensation is rarely applied as a means of remedy in these systems [12], [13]. The most cited paper on this topic is the paper of Hansen *et al* [13] where the effects of circuit inductances on the line current harmonics are clearly shown. The analytical analysis, however, is complex and the required reactance criteria not entirely clear. Furthermore, there is a noticeable absence in literature for analysing cases where the rectifier is directly connected to a fixed DC-voltage source.

In this paper, the focus is on a simple analytical calculation method for the design engineer to mitigate line current harmonics with passive compensation on the AC-side of a fixed DC-voltage source connected diode rectifier. Additionally, the required line reactance criteria is given, which is important for generator design. The passive compensation is done by considering the total reactance (internal generator reactance plus external added reactance) between the generator and the rectifier. This reactance is shown to have a significant effect on the lower order harmonic line currents. In this view, the attempt in the paper is to develop a systematic calculation method which determines the minimum reactance required to reduce the lower order line harmonic currents on the AC-side of the rectifier to less than a certain percentage of the fundamental. In addition to three-phase systems, the paper also considers five- and seven-phase systems. Multi-phase generators have several advantages over their three-phase counterpart, of which improved torque density and torque quality are the most important [11], [14].

The calculation method is also practically applied to two types of wind generators that are connected to stiff DC-voltage sources via a full-bridge diode rectifier. The measured line current waveforms are presented to show the effect of the passive harmonic current compensation.

II. SYSTEM DESCRIPTION

A block diagram of a diode rectifier connected wind generator system forming an interface to the DC-grid is shown in Fig. 1. With turbine rotation, there is a back EMF induced voltage in the generator. Between this induced voltage and the diode rectifier, there is impedance that consists of the generator's internal impedance and any external connected impedance. The DC-DC converter matches the variable diode rectifier output DC-voltage with the fixed DC-grid voltage

With a stiff DC-link voltage between the diode rectifier and the DC-DC converter, it is important to consider the voltage and current waveforms at the AC-side of the diode rectifier. These waveforms are strongly affected by the line inductance L of Fig. 1. If the line inductance is very small, then the phase voltage and line current waveforms are as shown in Fig. 2. However, if the line inductance is very large, then the phase voltage and line current waveforms are as shown in Fig. 3. It is clear that with a large line inductance, the line current harmonics are almost completely eliminated. At the same time though, a large line inductance

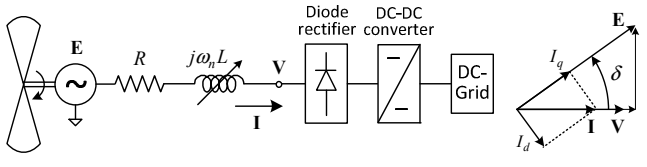

Fig. 1. DC-grid connected wind generator system and phasor diagram.

978-1-7281-4162-6/20/$31.00 ©2020 IEEE

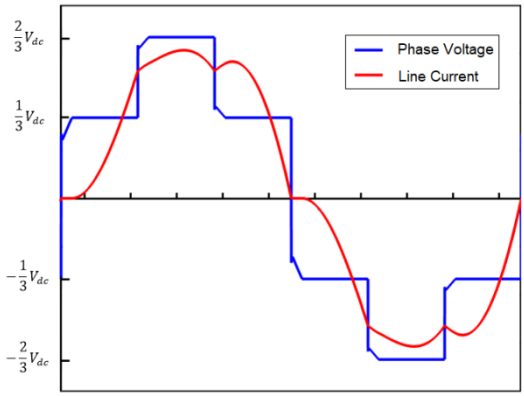

Fig. 2. Phase-voltage and line current waveforms at the AC-side of a 6-pulse diode rectifier with a small series line inductance.

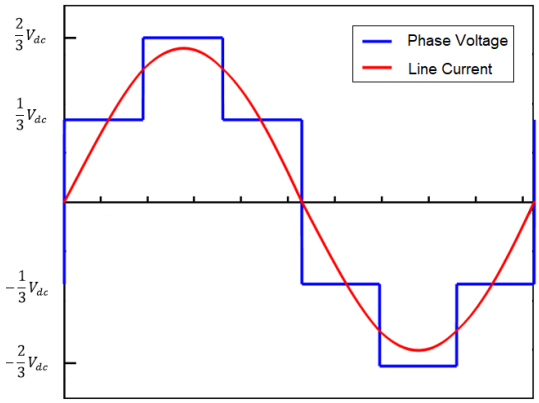

Fig. 3. Phase-voltage and line current waveforms at the AC-side of a 6-pulse diode rectifier with a large series line inductance.

leads to the ineffective use of the wind generator. This can be explained by considering the torque equation of a non-salient synchronous generator as

$$\tau = k\lambda_f I_q = k\lambda_f I\cos\delta\,. \qquad (1)$$

In (1), k is a machine constant, λ_f is the stator flux linkage due to the rotor field, I_q is the q-axis current and I the peak stator current as shown in the phasor diagram of Fig. 1. The load angle δ in (1) is defined in Fig. 1 and can be expressed by approximation as

$$\delta = \tan^{-1}\left(\frac{I_1\,\omega_1 L}{V_1}\right) = \tan^{-1}\left(\frac{I_1\,X_1}{V_1}\right)\quad [R\to 0]\,, \qquad (2)$$

where I_1 and V_1 are the respective RMS values of the fundamental line current and phase voltage, and ω_1 the fundamental angular frequency. From (2), it is clear that at per unit current and voltage, the load angle δ is a function of the line inductance L. Thus, the larger the line inductance, the larger δ becomes and the larger the drop in generator torque according to (1). If the generator torque is a requirement, then for a larger δ, a larger generator must be installed.

From the above discussion, it is clear that the design engineer must minimise the line inductance of the system subject to constraints imposed on the line current harmonic content. The aim of the paper is to generate information that can be useful to the design engineer.

III. Harmonic Analysis

In the paper the attempt is to develop a simple theoretical model for an n-pulse rectifier network connected to the DC-grid. An example of a 6-pulse rectifier is shown in Fig. 4. The model explicitly focusses on the per phase rectifier voltage, which, when referred from the DC-voltage source, can be expressed as a piecewise, discontinuous rectangular unction as shown in Fig. 3. Secondly, Fourier analysis is performed on the phase voltage waveform of Fig. 3 and each harmonic component is analysed. This approach is advantageous since it enables us to express the system as a series of simplified, equivalent circuits from which the line current can be evaluated on a harmonic basis.

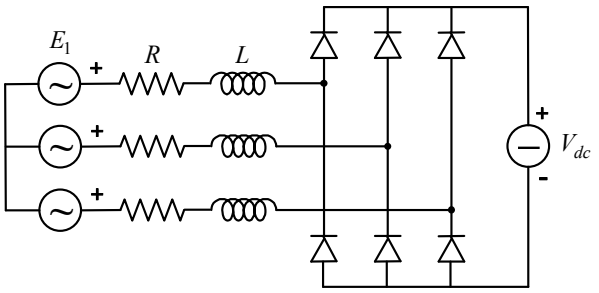

Fig. 4. Three-phase line commutated uncontrolled rectifier connected to a fixed DC-voltage source.

A. Analysis assumptions

The following assumptions are made in the harmonic analysis of the diode rectifier generator system:

1) The inductance and the resistance on the DC-side of the rectifier are small enough that they may be neglected, as shown in Fig. 4.

2) The forward conducting voltage drop across the diodes of the rectifier is small compared to the base voltages in the system and is therefore neglected; the diodes of the rectifier are thus taken as ideal.

3) The resistance of AC generators is usually in the order of 0.05 per unit. Therefore R in Fig. 4 is taken in the modelling as $R = 0.05$ per unit.

4) Generators are designed to have sinusoidal back EMF induced voltages, therefore the induced back EMF phase voltage waveforms of the generator in Fig. 4 are considered as perfect sinusoidal.

B. Harmonic equivalent circuits

With the above assumptions the system is modelled on a harmonic per phase equivalent circuit. The equivalent circuit for the fundamental (1st) harmonic is shown in Fig. 5(a). Here V_1 is the RMS voltage of the fundamental of the phase voltage at the AC phase-terminal of the rectifier. Furthermore, E_1 is the RMS value of the per-phase sinusoidal back EMF induced generator voltage. Hence the fundamental stator current can be calculated by

$$I_1 = \frac{\left|E_1\angle\delta - V_1\angle 0\right|}{\sqrt{R^2 + X_1^2}}\,, \qquad (3)$$

where $X_1 = \omega_1 L$ and ω_1 is the angular frequency of the fundamental voltage component.

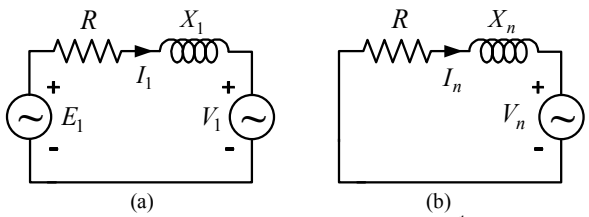

(a) (b)

Fig. 5. Equivalent circuits of (a) fundamental and (b) n^{th} harmonic.

Considering the harmonic equivalent circuit, we have from assumption 4) above that there are no induced back EMF harmonic voltages. Hence the higher order harmonic equivalent circuit becomes as shown in Fig. 5(b). Here V_n is the RMS voltage of the n^{th} order harmonic of the phase voltage at the AC phase-terminal of the rectifier. From this we can calculate the RMS value of the n^{th} order harmonic current as begin to format your paper, first write and save the content as

$$I_n = \frac{V_n}{\sqrt{R^2 + X_n^2}}, \tag{4}$$

where X_n is the n^{th} order harmonic reactance given by

$$X_n = \omega_n L = n\omega_1 L = nX_1 . \tag{5}$$

Using a simulation package the entire system of e.g. Fig. 4 for a certain load current I_l and certain line inductance L can be simulated. From this by Fourier series analysis of the simulated voltage waveform, the fundamental and harmonic voltages V_1 and V_n respectively can be determined. Knowing V_n, and X_n from (5), the harmonic currents can simply be calculated using (4). Of course, one can also do the harmonic analysis directly from the simulated line current waveform, which must give the same result as (4).

C. Approximate harmonic analysis

Using (4) is a fast way to calculate the harmonic current if the harmonic voltage is known. However, to obtain the harmonic voltage from full simulation for each considered case as explained above is computationally very inefficient. To improve on this we assume as an approximation that the phase voltage waveform always has the form of that shown in Fig. 3, i.e. of a system with a large series line inductance. In the next section the extent to which this approximation is valid is evaluated. With the approximated voltage waveform as in Fig. 3, the harmonic voltages of this waveform only need to be calculated once. With this known, all the harmonic currents can fast be calculated as a function of X_n.

For the three-phase 6-pulse rectifier case in Fig. 4, it is shown in the Appendix that the RMS values of the Fourier series harmonic voltages of the voltage waveform in Fig. 3 are given by

$$V_{n,3\varphi} = \frac{\sqrt{2}V_{dc}}{\pi n} \rightarrow n = 1, 5, 7, 11, 13, ... \tag{6}$$

This leads to the well-known equation for the fundamental (n = 1) RMS voltage of

$$V_{1,3\varphi} = \frac{\sqrt{2}V_{dc}}{\pi}. \tag{7}$$

Knowing (7), $I_{1,3\varphi}$ can be calculated from (3). Knowing (6), the harmonic currents for the three-phase case can be calculate from (4) and (5) as

$$I_{n,3\varphi} = \frac{V_{n,3\varphi}}{\sqrt{R^2 + (nX_1)^2}} \rightarrow n = 5, 7, 11, 13, ... \tag{8}$$

IV. Three-phase System Analysis Results

In this section the accuracy of the proposed approximate harmonic calculation method is evaluated against the actual harmonic currents of a three-phase 6-pulse rectifier system. In this comparison we work on a per unit basis where the fundamental voltage of (7) is taken as one per unit voltage. The per unit harmonic voltage of the approximate model is then from (6) and (7), given by

$$V_{n,3\varphi,\text{pu}} = \frac{1}{n} \rightarrow n = 5, 7, 11, 13, ... \tag{9}$$

The per unit harmonic current is then calculated from (8), with R = 0.05 per unit as per assumption 3), and (9) as

$$I_{n,3\varphi,\text{pu}} = \frac{1}{n\sqrt{0.05^2 + (nX_{1,\text{pu}})^2}} \rightarrow n = 5, 7, 11, 13, ... \tag{10}$$

In the comparison, the per unit line reactance $X_{1,\text{pu}}$ in (10) is varied between

$$0.05 \le X_1 \le 1.1 \text{ pu} . \tag{11}$$

To obtain the actual harmonic per unit values, the three-phase system of Fig. 4 is simulated in Matlab Simulink with the base values of the system as given in Table I. The base voltage in Table I was calculated according to (7). The simulation is done by always keeping the simulated fundamental line current at or close to 1.0 per unit current while varying X_l according to (11). For each X_l value, the harmonic line currents are determined from a harmonic Fourier series analysis of the simulated line current waveform. The per-unit RMS harmonic line currents are then calculated according to the base current value given in Table I.

From (6) and (8), it must be clear that the lower the harmonic order, the larger the expected harmonic line current. Hence, for the three-phase system we focus only on the per unit value of the 5th harmonic line current as this current is the largest higher-order harmonic current. The simulated and the proposed approximate-harmonic calculated results of the 5th harmonic of the three-phase system are shown in Fig. 6. From this, four important deductions are made for the three-phase system:

(i) The approximate-harmonic calculation according to (9) and (10) gives a very good prediction of the 5th harmonic current for line reactance values as low as 0.3 per unit. It also gives a conservative prediction as the actual harmonic current is always equal to or less than the predicted harmonic current. Thus, using (9) and (10), the designer knows that for a chosen line reactance the actual harmonic per unit currents will always we equal or less than calculated.

(ii) To have the per unit harmonic currents less than 0.1 per unit (less than 10 %), the line reactance according to Fig. 7 must be $X_1 > 0.4$ per unit. If required to be less than 0.05 per unit (less than 5 %), then $X_1 > 0.8$ per unit. So these are line reactance values which the design engineer can now use without any calculation to ensure that the harmonic content is within limits. The line current waveforms with X_1 = 0.4 per unit and X_1 = 0.8 per unit are shown in Fig. 7. These current waveforms can be used and further investigated by the design engineer to see what effect it has on the torque ripple and noise of the generator.

(iii) The importance of the outcome of the values X_1 = 0.4

TABLE I. Parameter Base Values Of Simulated System

Parameter	Base value
f_{base}	50 Hz
V_{dc}	100 V
S_{base}	4.05 kVA
$V_{ph,base}$	45.0 V
I_{base}	30.0 A
Z_{base}	1.50 Ω
L_{base}	4.775 mH

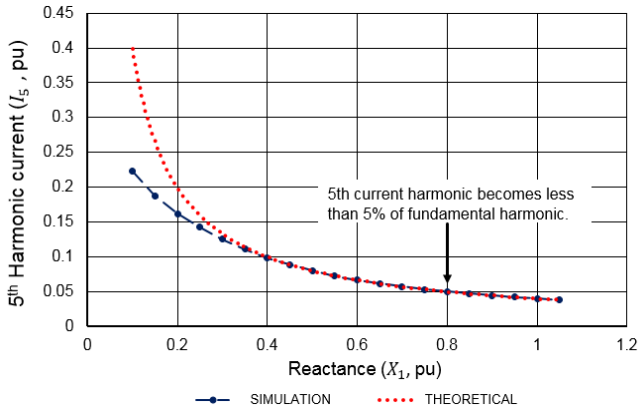

Fig. 6. Per unit 5th harmonic current versus per unit line reactance of three-phase system.

per unit and X_1 = 0.8 per unit cannot be underestimated, because these per unit values are typical synchronous reactance per unit values of permanent magnet and wound-field synchronous machines respectively. This implies that no external line reactance may be required to be put in series with the synchronous wind generator; there is further the opportunity for the design engineer to design the synchronous generator according to these reactance values.

(iv) With X_1 = 0.4 per unit and X_1 = 0.8 per unit, the corresponding load angles δ at unity line current and -line voltage can be calculated from (2). From this the cos δ values can be determined with the results summarised in Table II. The effect the cos δ values of Table II has on the torque capability of the generator can be determined from (1); that is with X_1 = 0.4 per unit a 7 % drop in torque density is caused and with X_1 = 0.8 per unit a 22 % drop in torque density. These drops in torque densities have to be considered by the designer in the design stage of the generator. Nevertheless, despite the drop in generator torque, the study shows that the effect of the line reactance for minimum harmonic content is not large.

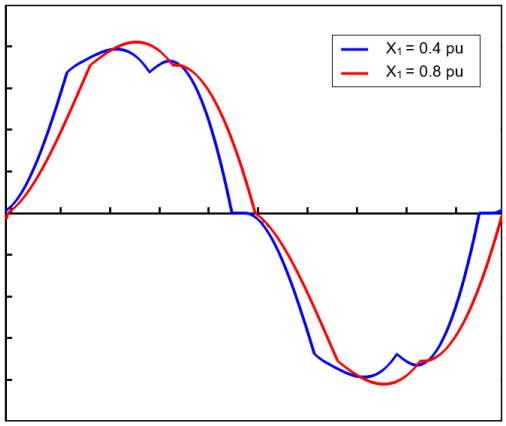

Fig. 7. Three-phase line current waveforms with X_1 = 0.4 per unit and X_1 = 0.8 per unit.

TABLE II. COS Δ CALCULATIONS VERSUS X_1 PER UNIT VALUES.

X_1 per unit	δ °	cos δ
0.4	21.8	0.93
0.8	38.7	0.78

V. MULTI-PHASE SYSTEMS

In this section five- and seven-phase diode rectifier generator systems are investigated in terms of the line current harmonic content. As shown by (20) and (21) in the Appendix, (9) and (10) for the three-phase system are also valid for five- and seven-phase systems, with the only difference the harmonic orders. The per unit harmonic currents for five- and seven-phase systems are thus respectively given by

$$I_{n,5\varphi,\mathrm{pu}} = \frac{1}{n\sqrt{0.05^2 + (nX_{1,\mathrm{pu}})^2}} \rightarrow n = 3,\ 7,\ 9,\ 11,\ 13,\ \ldots \quad (12)$$

and

$$I_{n,7\varphi,\mathrm{pu}} = \frac{1}{n\sqrt{0.05^2 + (nX_{1,\mathrm{pu}})^2}} \rightarrow n = 3,\ 5,\ 9,\ 11,\ 13,\ \ldots \quad (13)$$

The comparisons between the approximate-analytical results according to (12) and (13) and the actual-simulated results of the per unit harmonic current versus line reactance are shown in Figs. 8 and 9 for the five- and seven-phase machines respectively. In both these cases the 3rd harmonic line current is investigated, as this is the largest harmonic current according to (12) and (13).

From Figs. 9 and 10, it is firstly observed that there is no difference in the approximate analysis results of the five- and seven-phase systems, as expected from (12) and (13). Secondly, as for the three-phase system there is a very good comparison between the approximate analysis results of (12) and (13) and the actual-simulated results for reactance values as low as, say, X_1 = 0.3 per unit. The important difference between the five- and seven-phase system results and those of the three-phase system, is the factor 5/3 = 1.67 larger reactance needed for the five- and seven-phase systems to have the 3rd harmonic current less than 10 % and 5 % of the fundamental, that is with X_1 = 0.67 per unit and X_1 = 1.33 per unit respectively.

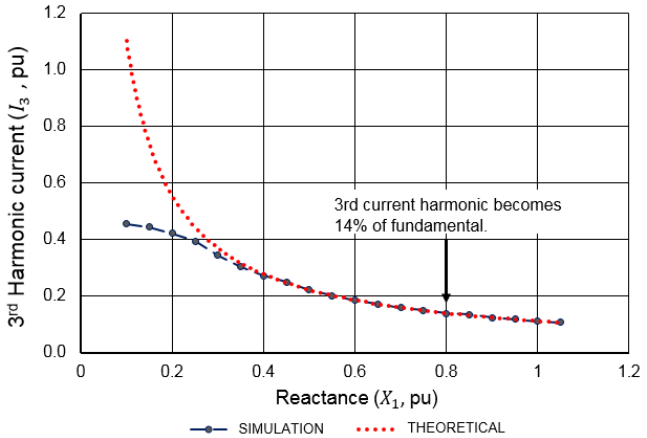

Fig. 8. Per unit 3rd harmonic current versus per unit line reactance of five-phase system.

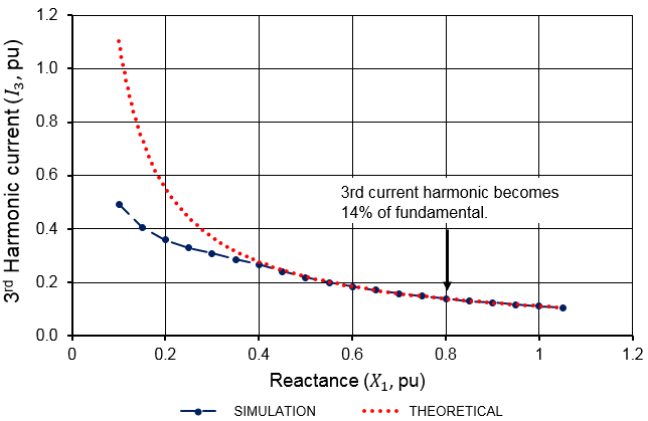

Fig. 9. Per unit 3rd harmonic current versus per unit line reactance of seven-phase system.

To compare the phase voltage and line current waveforms with those of the three-phase system, the waveforms of the five- and seven-phase systems are shown in Figs. 10 and 11 for the case where X_1 = 0.8. The effect of the 3rd harmonic current is clearly visible in both current waveforms, which is in contrast with the three-phase current waveform of Fig. 7. The voltage waveforms of Figs. 10 and 11 are the classical phase-voltage waveforms when the line reactance is relatively large. These waveforms are assumed in the derivations in the Appendix and in (12) and (13).

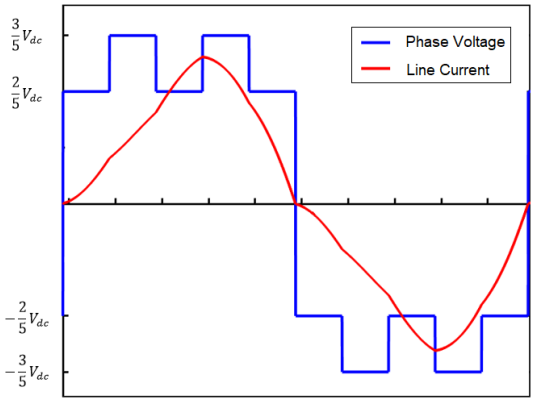

Fig. 10. Phase-voltage and line current waveforms at the AC-side of a 10-pulse diode rectifier with X_1 = 0.8 per unit.

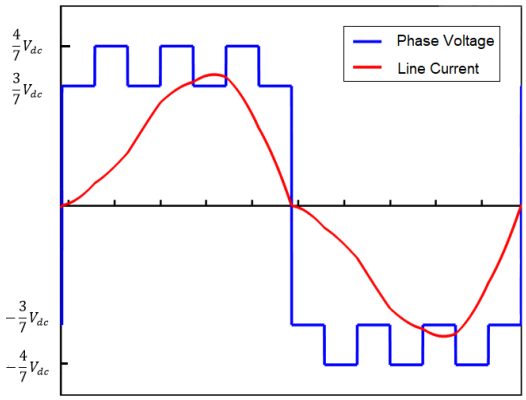

Fig. 11. Phase-voltage and line current waveforms at the AC-side of a 14-pulse diode rectifier with X_1 = 0.8 per unit.

VI. Measured Results

The accuracy of the theoretical model is compared to practical cases of two PM generators that are connected to stiff DC-voltage sources via a 6-pulse diode rectifier. The one generator is a 2.2 kW, 6-pole, geared PM wind generator shown in Fig. 12(a). The other generator is a 4.2 kW, 28-pole, direct-drive PM wind generator shown in Fig. 12(b). The circuit parameters and testing data of the generators are given in Table III. The measured line current waveforms with and without passive compensation of both generators are shown in Figs. 13 and 14.

The analytically predictive harmonic currents given in Table III do compare in general well with the given measured results of both 6-pole and 28-pole wind generators. The line current waveforms of the 6-pole generator in Fig. 13 show that compensation is hardly necessary due to the relatively large 21 mH synchronous inductance. By adding a small external inductance of 3 mH, shapes the current further to be more sinusoidal. The uncompensated line current waveform of the 28-pole generator in Fig. 14 has relatively large 5th and 7th harmonic currents as shown in Fig. 15. By

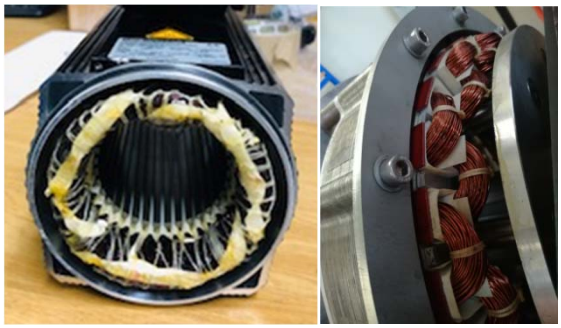

(a) (b)

Fig. 12. Photos of (a) 6-pole, overlap winding PM generator with outer diameter = 105 mm, and (b) 28-pole, non-overlap winding PM generator with outer diameter = 384 mm.

TABLE III. Measured And Calculated 5th And 7th Harmonic Currents With And Without Compensation.

Generator	f (Hz)	R (Ω)	L (mH)	X_1 (Ω)	V_{dc} (V)	I_1 (A)	I_5 (A) Meas.	I_5 (A) Anal.	I_7 (A) Meas.	I_7 (A) Anal.
6-pole	35.6	1.15	21	4.7	78	2.05	0.437	0.298	0.144	0.152
6-pole	31.1	1.15	21	4.1	52	6.33	0.447	0.228	0.261	0.116
6-pole-C	43.3	1.15	24	6.53	52	6.02	0.17	0.143	0.064	0.073
28-pole	39.8	0.13	0.9	0.23	62	31	5.0	4.923	2.27	2.52
28-pole-C	74.9	0.14	2.4	1.13	58	39	1.6	0.925	0.3	0.472

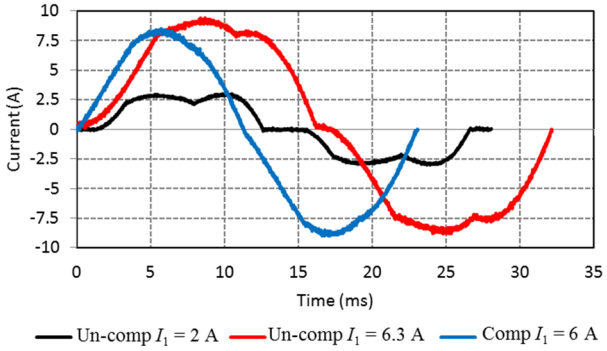

Fig. 13. Line current waveforms with and without passive compensation of the three-phase diode rectifier connected 6-pole PM wind generator.

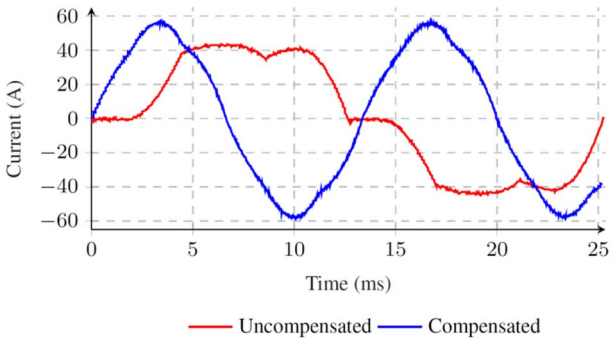

Fig. 14. Line current waveforms with and without passive compensation of the three-phase diode rectifier connected 28-pole PM wind generator.

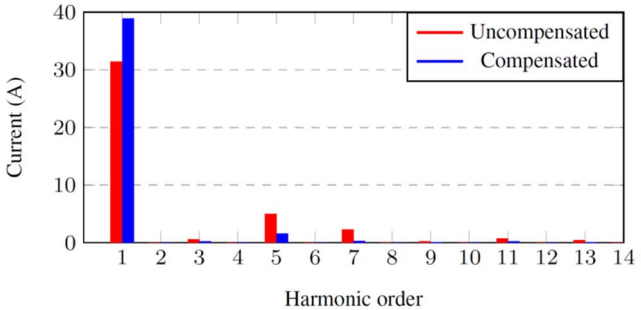

Fig. 15. Measured current harmonics with and without passive compensation of the 28-pole PM wind generator.

increasing the line inductance from 0.9 mH to 2.4 mH drastically reduces the current harmonics as shown in Fig. 15, resulting in a very much sinusoidal current waveform as shown in Fig. 14.

VII. Conclusion

In this paper the effect of the line reactance on the current harmonic content of generators that are connected directly to DC-grids via diode rectifiers is considered. The following conclusions are drawn from the results in the paper i.e. for sinusoidal designed (thus not brushless dc) generators:

- It is shown that the proposed simple analytical method is fast and can be used very effectively for the prediction of the harmonic line currents of the generator. This is very valuable for the designer in the design stage of the generator.

- A significant outcome of the study shows that the required minimum per unit line reactance for minimising the large low order harmonic currents lies in the typical per unit synchronous reactance range of synchronous generators. This implies that an externally connected reactance may not be necessary, or else the generator can be designed for a higher synchronous reactance.

- Passive harmonic current compensation in five- and seven-phase systems is shown to have no advantage compared to the three-phase system. The reason for this is the large 3rd harmonic current in these generator systems.

Appendix

The voltage waveform of Fig. 3 for the three-phase system can be expressed mathematically by a Fourier series as

$$v(\theta) = \sum_n a_n \sin(n\theta) + \sum_n b_n \cos(n\theta)\,, \qquad (14)$$

where n is the harmonic order and a_n and b_n the Fourier harmonic coefficients. By inspection of the waveform of Fig. 3 it can be observed that $v(-\theta) = -v(\theta)$, which means b_n in (14) is $b_n = 0$, and that $v(\theta + \pi) = -v(\theta)$, which means there are no even harmonics. For the three-phase system there will also be no harmonics that are multiples of 3. Hence, we can express from (14) the harmonic voltage and the RMS value of the harmonic voltage as follows:

$$v_n(\theta) = a_n \sin(n\theta) \;\rightarrow n = 1,\ 5,\ 7,\ 11,\ 13 \ldots \qquad (15)$$

$$V_{n,3\varphi} = \frac{a_n}{\sqrt{2}} \;\rightarrow n = 1,\ 5,\ 7,\ 11,\ 13 \ldots \qquad (16)$$

The voltage wave of Fig. 3 is a quarter-wave symmetrical function so that the harmonic coefficient a_n can be determined by integrating only from 0 to π/2 as

$$a_n = \frac{4}{\pi} \int_0^{\pi/2} v_n(\theta) \sin(n\theta)\, d\theta\,. \qquad (17)$$

Applying (17) to the voltage wave of Fig. 3 we find

$$a_n = \frac{4}{\pi}\left[\int_0^{\pi/3} \tfrac{1}{3} V_{dc} \sin(n\theta)\, d\theta + \int_{\pi/3}^{\pi/2} \tfrac{2}{3} V_{dc} \sin(n\theta)\, d\theta \right] = \frac{2V_{dc}}{\pi n}. \qquad (18)$$

From (16) and (18) the RMS harmonic voltage is given by

$$V_{n,3\varphi} = \frac{\sqrt{2}V_{dc}}{\pi n} \;\rightarrow n = 1,\ 5,\ 7,\ 11,\ 13, \ldots \qquad (19)$$

It is important to note that exactly the same result of (19) is obtained for five- and seven-phase systems if their voltage waveforms, shown in Figs. 11 and 12, are considered, with the only difference in the harmonic orders, that is

$$V_{n,5\varphi} = \frac{\sqrt{2}V_{dc}}{\pi n} \;\rightarrow n = 1,\ 3,\ 7,\ 9,\ 11, \ldots \qquad (20)$$

$$V_{n,7\varphi} = \frac{\sqrt{2}V_{dc}}{\pi n} \;\rightarrow n = 1,\ 3,\ 5,\ 9,\ 11, \ldots \qquad (21)$$

References

[1] V. Yaramasu, B. Wu, P. C. Sen, S. Kouro and M. Narimani, "High-power wind energy conversion systems: state-of-the-art and emerging technologies," Proceedings of the IEEE, vol. 103, no. 5, pp 740–788, May 2015.

[2] H. Wang and M. A. Redfern, "The advantages and disadvantages of using HVDC to interconnect AC networks," 45th International Universities Power Engineering Conference (UPEC), Cardiff (United Kingdom), pp 1–5, 2010.

[3] S. Seman, R. Zurowski and C. Taratoris, "Interconnection of advanced type 4 WTGs with diode rectifier based HVDC solution and weak AC grids," Proceedings of the 14th Wind Integration Workshop, Brussels, (Belgium), 20–22 Oct., 2015.

[4] R. Li, L. Yu, L. Xu and G. P. Adam, "DC fault protection of diode rectifier unit based HVDC system connecting offshore wind farms," IEEE Power & Energy Society General Meeting (PESGM), Portland, OG (USA), 5–10 Aug., 2018.

[5] P. Huynh, P. Wang, and A. Banerjee, "An integrated permanent-magnet-synchronous-generator-rectifier architecture for limited-speed-range applications," in IEEE Energy Conversion Congress and Exposition (ECCE), Portland, OG (USA), pp 3413–3420, Sep. 2018.

[6] M. S. U. Khan, A. I. Maswood, K. Satpathi, M. T. Iqbal and A. Tripathi, "Analysis of brushless wound rotor synchronous generator with unity power factor rectifier for series offshore DC wind power collection," 44th Annual Conference of the IEEE Industrial Electronics Society (IECON), Washington, DC (USA), pp 1693–1698, 2018.

[7] M. Pape and M. Kazerani, "On the efficiency of series-connected offshore DC wind farm configurations", IEEE Energy Conversion Congress and Exposition (ECCE), Baltimore, MD (USA), pp 921–926, Oct. 2019.

[8] Y. Xia, K. H. Ahmed and B. W. Williams, "Different torque ripple reduction methods for wind energy conversion systems using diode rectifier and boost converter" 2011 IEEE International Electric Machines and Drives Conference (IEMDC), Niagara Falls (Canada), pp. 729– 734, 2011.

[9] M. Stiebler, "PM synchronous generator with diode rectifier for wind systems using FACTS compensators," International Symposium on Power Electronics, Electrical Drives, Automation and Motion, pp 1295–1300, 2012.

[10] H. Kim, J. Sastry, J. Niiranen and D. Pan, "Active compensator augmented diode bridge rectifier wind system," 39th Annual Conference of the IEEE Industrial Electronics Society (IECON), Vienna (Austria), pp 5230–5235, Nov., 2013.

[11] M. I. Masoud, "Five-phase uncontrolled line commutated rectifier: AC side compensation using shunt active power filter," Proceedings of the 8th GCC Conference & Exhibition, Muscat (Oman), 1–4 Feb., 2015.

[12] M. Sakui, H. Fujita and M. Shioya, "A method for calculating harmonic currents of a three-phase bridge uncontrolled rectifier with DC filter," IEEE Transactions on Industrial Electronics, vol. 36, no. 3, pp 434–440, Aug., 1989.

[13] S. Hansen, L. Asiminoaei and F. Blaabjerg, "Simple and advanced methods for calculating six-pulse diode rectifier line-side harmonics," 38th IAS Annual Meeting Conference Record of the Industry Applications Conference, Salt Lake City, UT (USA), vol. 3, pp. 2056–2062, 2003.

[14] N. E. A. Hassanain and J. E. Fletcher, "Steady-state performance assessment of three- and five-phase permanent magnet generators connected to a diode bridge rectifier under open-circuit faults," IET Renewable Power Generation, vol. 4, no. 5, pp. 420–427, 2010.